World Academy of Science, Engineering and Technology
International Journal of Electrical and Computer Engineering
Vol:10, No:5, 2016

Active Islanding Detection Method Using Intelligent Controller

Kuang-Hsiung Tan, Chih-Chan Hu, Chien-Wu Lan, Shih-Sung Lin, Te-Jen Chang

***Abstract*—**An active islanding detection method using disturbance signal injection with intelligent controller is proposed in this study. First, a DC\AC power inverter is emulated in the distributed generator (DG) system to implement the tracking control of active power, reactive power outputs and the islanding detection. The proposed active islanding detection method is based on injecting a disturbance signal into the power inverter system through the *d*-axis current which leads to a frequency deviation at the terminal of the *RLC* load when the utility power is disconnected. Moreover, in order to improve the transient and steady-state responses of the active power and reactive power outputs of the power inverter, and to further improve the performance of the islanding detection method, two probabilistic fuzzy neural networks (PFNN) are adopted to replace the traditional proportional-integral (PI) controllers for the tracking control and the islanding detection. Furthermore, the network structure and the online learning algorithm of the PFNN are introduced in detail. Finally, the feasibility and effectiveness of the tracking control and the proposed active islanding detection method are verified with experimental results.

***Keywords*—**Distributed generators, probabilistic fuzzy neural network, islanding detection, non-detection zone.

I. Introduction

ISLANDING detection is an essential protection requirement for distributed generators (DGs) for personnel and equipment safety. The islanding phenomenon for the DG is defined when the DG continues to operate with local loads when the utility power is disconnected [1]. The islanding phenomenon usually occurs when the load power and the output power of the DG are balanced, i.e., the load power is entirely supplied by the DG. At this time, if the utility power is failed or interrupted, the disturbances of frequency and voltage of the DGs cannot be detected with the standard of IEEE1547or UL1741 [2], [3]. The islanding phenomenon will damage the power systems and the safety of maintenance staffs. Thus, all DG equipment is required to present an effective islanding detection method [4].

In the past decade, many literatures [5]-[8] have been proposed to prevent islanding phenomenon caused by DGs. In [5], the active frequency drift method was proposed to add dead time into the output current of the power inverter and resulted in current and voltage distortion at the point of common coupling (PCC). Thus, when the utility power is failed or interrupted, the frequency can drift beyond the non-detection zone (NDZ). In [6], the proposed active islanding detection method is based on injecting a negative-sequence current through the power inverter by means of unified three-phase signal processor. The signal cross-correlation index between the injected reactive power and the frequency deviation at the PCC is proposed to detect the islanding phenomenon in [7]. A positive feedback anti-islanding scheme using *q*-axis injection method was proposed. The method injects a disturbance signal, which contains the difference of terminal voltage, into the active power axis (*q*-axis). When the utility power is failed or interrupted, it can accelerate the voltage to drift beyond the NDZ [8]. However, the proposed method is based on the active power disturbance method for islanding detection which inherently has larger NDZ compared with the reactive power disturbance method for islanding detection [9].

Recently, the study about the integration of artificial neural network and fuzzy has been proposed in many research fields. The fuzzy neural network (FNN) owns the abilities of prediction, modeling, training, and solving problems with uncertainty [10]. Moreover, FNN does not require mathematical models and has the ability to approximate nonlinear systems [11]. Furthermore, nowadays, the new intelligent controllers, probabilistic neural network (PNNs), have also been proposed in the literatures [12]-[15]. The PNN is a feed-forward neural network and is a direct neural network implementation of Bayes classification rule and Parzen nonparametric probability density function (PDF) estimation [12]. In addition, the PNN has an inherent parallel structure, a fast training process, and guaranteed optimal classification performance if a sufficiently large training set is provided [13]. Therefore, the PNN can handle the uncertainties in industry applications effectively, and it has been widely used in nonlinear mapping, pattern classification, and classification and fault detection [14], [15]. Owing to the above advantages of PNN and FNN, the PFNN, which integrates the characteristics of PNN and FNN, has been proposed in some applications, such as stochastic modeling and control problems. In [16], the PFNN is capable of solving the uncertainties in industry applications.

In this study, a grid-connected three-phase DG system using the adopted PFNN controllers is researched for the tracking control and the islanding detection. First, a DC source power inverter is emulated the DG system to implement the tracking control of active power, reactive power outputs and the

C. C. Hu is with System Manufacturing Center, National Chung-Shan Institute of Science and Technology, Sanxia District, New Taipei City 23742, Taiwan (e-mail: huchihchan@gmail.com).

K. H. Tan is with the Department of Electrical and Electronic Engineering, Chung Cheng Institute of Technology, National Defense University, Taoyuan 335, Taiwan (corresponding author; phone: +886-3-380-9991 ext.128; e-mail: s913115@gmail.com).

C. W. Lan, S. S Lin and T. J. Chang are with the Department of Electrical and Electronic Engineering, Chung Cheng Institute of Technology, National Defense University, Taoyuan 335, Taiwan (e-mail: g941339@gmail.com; shihsunglin@gmail.com; karl591218@gmail.com).

islanding detection. Then, the characteristics of the NDZ and the proposed active islanding detection method using disturbance signal injection are introduced in detail. Moreover, the PFNNs are adopted to replace the traditional PI controllers for the tracking control and the islanding detection to improve the transient and steady-state responses of the active power and reactive power outputs of the power inverter, and the performance of the islanding detection method. Furthermore, the training algorithm based on backpropagation (BP) is derived to train the connective weights, means, and standard deviations of the membership functions in the adopted PFNN online. Finally, the adopted PFNN controllers to control the active power and reactive power outputs of the power inverter and to detect the islanding phenomenon is realized in a personal computer (PC)-based control computer via MATLAB & Simulink, and the effectiveness is verified by experimentation.

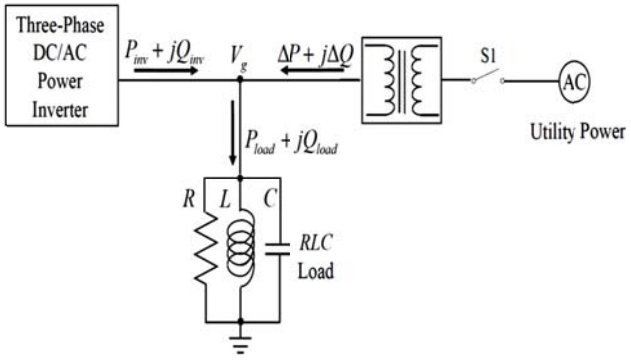

Fig. 1 Test circuit with parallel RLC load

II. Active Islanding Detection Method

A. Non-Detection Zone

The NDZ is derived from the test circuit with a parallel *RLC* resonant tank as the load as shown in Fig 1. The power flow relations of the inverter active power P_{inv}, reactive power Q_{inv}, *RLC* load active power P_{load}, reactive power Q_{load}, and utility active power ΔP, reactive power ΔQ are as follows:

$$P_{inv} = P_{load} - \Delta P;\ Q_{inv} = Q_{load} - \Delta Q. \tag{1}$$

It is difficult to detect the islanding phenomenon when active power and reactive power outputs of the grid-connected power inverter are equal to the active and reactive power of the *RLC* load, i.e., $\Delta P = 0$, $\Delta Q = 0$ [17]. When the utility power is disconnected, the added disturbance signal in the *d*-axis current will result in $Q_{inv} \neq 0$. It can be obtained as;

$$Q_{inv} = V_g^2(\frac{1}{\omega_g L} - \omega_g C) = P_{load} R(\frac{1}{\omega_g L} - \omega_g C), \tag{2}$$

where ω_g is the angular frequency of the utility power; V_g is the terminal *rms* voltage of *RLC* load. Moreover, the quality factor is defined as;

$$Q_f = R\sqrt{\frac{C}{L}} \tag{3}$$

Substitute (3) into (2), then (2) can be rewritten as follows:

$$\frac{Q_{inv}}{P_{load}} = Q_f(\frac{1}{\omega_g \sqrt{LC}} - \omega_g \sqrt{LC}). \tag{4}$$

Since the resonant frequency ω_o equals $\sqrt{1/LC}$, (4) can be rewritten as follows:

$$\frac{Q_{inv}}{P_{load}} = Q_f(\frac{\omega_o}{\omega_g} - \frac{\omega_g}{\omega_o}) = Q_f(\frac{f_o}{f_g} - \frac{f_g}{f_o}), \tag{5}$$

where f_g and f_o are the frequency of ω_g and ω_o. The NDZ is obtained with the maximum and minimum frequency defined in the IEEE Standard 1547 [2] as follows:

$$Q_f(\frac{f_{min}}{f_g} - \frac{f_g}{f_{min}}) \le \frac{Q_{inv}}{P_{load}} \le Q_f(\frac{f_{max}}{f_g} - \frac{f_g}{f_{max}}), \tag{6}$$

where $f_{\max}$ and f_{min} are the maximum and minimum frequency thresholds; $Q_f(\frac{f_{min}}{f_g} - \frac{f_g}{f_{min}})$ is the lower limit of the NDZ; $Q_f(\frac{f_{max}}{f_g} - \frac{f_g}{f_{max}})$ is the upper limit of NDZ.

B. Active Islanding Detection Method Using Disturbance Signal Injection

The proposed active islanding detection method is based on injecting a disturbance signal into the power inverter system through the *d*-axis current as shown in Fig. 2, where P_{inv}^* is the active power command of the power inverter; Q_{inv}^* is the reactive power command of the power inverter; θ is the synchronous angle obtained by phase loop lock (PLL); i_{de}^* and i_{qe}^* are the *d-q* axes current commands; i_{us}^*, i_{vs}^*, i_{us}^* are three-phase current commands. The errors of active power and reactive power are regulated by the PI or PFNN controllers to obtain the *d-q* axes current commands. Then, using the coordinate transformation algorithm, three-phase current commands can be generated. The *d*-axis current command i_{de}^* consists of *d*-axis current i_{de} and injected disturbance signal i_{dist}. The magnitude of the injected disturbance signal i_{dist} becomes stronger when the utility power is disconnected. The injected disturbance signal i_{dist} is designed as:

$$i_{dist} = k sign(\Delta f),\ sign(\Delta f) = \begin{Bmatrix} 1, & f[k] > f[k-1] \\ 0, & f[k] = f[k-1] \\ -1, & f[k] < f[k-1] \end{Bmatrix} \tag{7}$$

where k is the gain of disturbance signal; *sign* is the sign function, and $sign(\Delta f)$ is determined by the frequency difference of current and last samples.

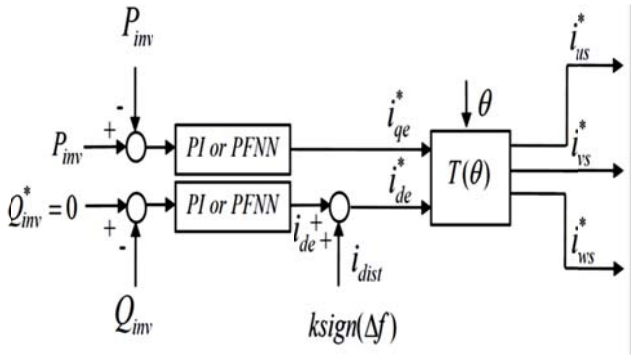

Fig. 2 Control block of proposed islanding detection method

The proposed active islanding detection method can push the frequency of the power inverter f to drift beyond the NDZ by adding the disturbance signal i_{dist} in the *d*-axis current i_{de} when the utility power is disconnected.

III. Probabilistic Fuzzy Neural Network Controller

Though the PI control has the advantages of simple structure and is easily implemented, the traditional PI controller is not robust in dealing with system uncertainties such as modeling errors, parameter variations and external disturbances in practical applications. Hence, in order to achieve superior effect for the proposed active islanding detection method, the online trained PFNN controllers are adopted to replace the traditional PI controllers to achieve further rapid response of the islanding detection and improve the transient and steady-state responses of the active power and reactive power outputs of the power inverter.

A. Network Structure

The adopted five-layer of the PFNN is illustrated in Fig. 3, which consists of the input layer, the membership layer, the probabilistic layer, the rule layer and the output layer. Moreover, the signal propagation and the basic function of each layer are described in detail as follows:

1. Input layer (layer 1): For every node in this layer, the node input and the node output are obtained as:

$$x_i(N) = e_i(N), \quad i = 1, 2 \tag{8}$$

where x_i represents the *i*th input to the input layer; *N* represents the *N*th iteration. The inputs of the PFNN are $e_1(N) = e$ and $e_2(N) = \dot{e}$, which are the tracking error and its derivative, respectively. These nodes only pass the input signal to the next layer. In this study, the input variables are $e = P^*_{inv} - P_{inv}$ for the active power control and $e = Q^*_{inv} - Q_{inv}$ for the reactive power control.

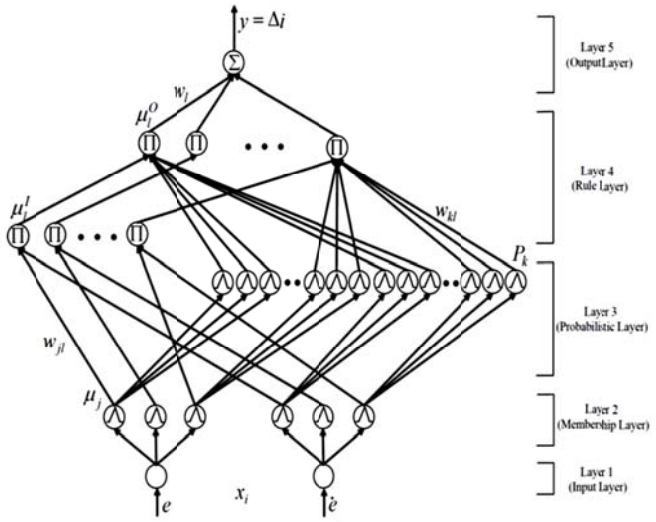

Fig. 3 Network structure of PFNN

2. Membership layer (layer 2): In this layer, the receptive field function is usually a Gaussian function in FNN. In order to reduce the computational requirements, a triangular function $f_m(x_i)$ is selected as the receptive field function. The equations of the triangular function $f_m(x_i)$ are provided as:

$$\mu_j(x_i) = f_m(x_i) = \begin{cases} 0 & if \quad x_i \ge m_j + \sigma_j,\ x_i \le m_j - \sigma_j \\ \dfrac{x_i - m_j + \sigma_j}{\sigma_j} & if \quad m_j - \sigma_j < x_i \le m_j \\ \dfrac{-x_i + m_j + \sigma_j}{\sigma_j} & if \quad m_j < x_i \le m_j + \sigma_j \end{cases} \tag{9}$$
$$i = 1, 2. \qquad j = 1, 2, \ldots, 6.$$

where $\mu_j(x_i)$ is the output of the *j*th node of the *i*th input variable; σ_j is the center's width of the triangle; m_j is the center of the triangle.

3. Probabilistic layer (layer 3): For the same reason in membership layer, another triangular function $f_p(\mu_j)$ is designed as the receptive field function and its equations are provided as:

$$P_k(\mu_j) = f_p(\mu_j) = \begin{cases} 0 & if \quad \mu_j \ge m_k + \sigma_k,\ \mu_j \le m_k - \sigma_k \\ \dfrac{\mu_j - m_k + \sigma_k}{\sigma_k} & if \quad m_k - \sigma_k < \mu_j \le m_k \\ \dfrac{-\mu_j + m_k + \sigma_k}{\sigma_k} & if \quad m_k < \mu_j \le m_k + \sigma_k \end{cases} \tag{10}$$
$$k = 1, 2, \ldots, 18$$

where $P_k(\mu_j)$ is the output of the *k*th node of the *j*th input variable; σ_k is the center's width of the triangle; m_k is the center of the triangle.

4. Rule layer (layer 4): In this layer, each node corresponds to a rule in the knowledge base. In the Mamdani inference, the node itself performs the product operation to obtain the inference set according to the rules as shown in (11). The probabilistic information is processed using the Bayes'

theorem [12] in consideration of the group of fuzzy grade being independent variables as shown in (12). Thus, the input and the output of this layer are described as:

$$\mu_l^I = \prod_j w_{jl}\mu_j \tag{11}$$

$$P_l^I = \prod_k w_{kl}P_k \tag{12}$$

$$\mu_l^O = \mu_l^I P_l^I \qquad l = 1, 2, \ldots, 9. \tag{13}$$

where P_l^I and μ_l^I are the input of rule layer; w_{kl} is the connective weight between the probabilistic layer and the rule layer which is set to be 1; w_{jl} is the connective weight between the membership layer and the rule layer, which is also set to be 1; μ_l^O is the output of the rule layer.

5. output layer (layer 5): In this layer, the input and the output of the node are obtained as:

$$y(N) = \Delta i = \sum_{l=1}^{9} w_l \mu_l^O \tag{14}$$

where $y(N) = \Delta i$ is the output of the PFNN; w_l is the connective weight between the rule layer and the output layer.

B. Online Learning Algorithm

According to the supervised learning algorithm, the parameter learning can be achieved by online regulate the connective weights between the output layer and rule layer, and the mean and standard deviation of the membership functions using the BP algorithm to minimize a given energy function. Hence, in order to describe the online learning algorithm of the PFNN, first the energy function E is defined as:

$$E = \frac{1}{2}(P_{inv}^* - P_{inv})^2 = \frac{1}{2}e^2 \tag{15}$$

Then, the update rules for the parameters in the PFNN are introduced as follows:

1. Layer 5: In this layer, the error term to be propagated is computed as:

$$\delta_o = -\frac{\partial E}{\partial y(N)} = -\frac{\partial E}{\partial P_{inv}}\frac{\partial P_{inv}}{\partial y(N)} \tag{16}$$

By using the chain rule, the connective weights are updated by the amount:

$$\Delta w_l = -\eta_1 \frac{\partial E}{\partial w_l} = -\eta_1 \frac{\partial E}{\partial y(N)}\frac{\partial y(N)}{\partial w_l} = \eta_1 \delta_o \mu_l^O \tag{17}$$

where the factor η_1 is the learning rate. The connective weight w_l is updated by the followings:

$$w_l(N+1) = w_l(N) + \Delta w_l \tag{18}$$

2. Layer 4: In this layer, the error terms to be propagated are described as:

$$\delta_l = -\frac{\partial E}{\partial \mu_l^O} = -\frac{\partial E}{\partial y(N)}\frac{\partial y(N)}{\partial \mu_l^O} = \delta_o w_l \tag{19}$$

3. layer 2: The error terms to be propagated are obtained by:

$$\delta_j = -\frac{\partial E}{\partial \mu_j} = -\frac{\partial E}{\partial y(N)}\frac{\partial y(N)}{\partial \mu_l^O}\frac{\partial \mu_l^O}{\partial \mu_l^I}\frac{\partial \mu_l^I}{\partial \mu_j} = \sum_l \delta_l P_l^I \tag{20}$$

By using of the chain rule, the update laws of center and center's width of the triangle are computed as follows:

$$\begin{aligned}\Delta m_j &= -\eta_2 \frac{\partial E}{\partial m_j} = -\eta_2 \frac{\partial E}{\partial y(N)}\frac{\partial y(N)}{\partial \mu_l^o}\frac{\partial \mu_l^o}{\partial \mu_l^I}\frac{\partial \mu_l^I}{\partial \mu_j}\frac{\partial \mu_j}{\partial m_j} \\ &= \begin{cases} -\eta_2 \delta_j \dfrac{1}{\sigma_j} & if \quad m_j - \sigma_j < x_i \le m_j \\ \eta_2 \delta_j \dfrac{1}{\sigma_j} & if \quad m_j < x_i \le m_j + \sigma_j \end{cases}\end{aligned} \tag{21}$$

$$\begin{aligned}\Delta \sigma_j &= -\eta_3 \frac{\partial E}{\partial \sigma_j} = -\eta_3 \frac{\partial E}{\partial y(N)}\frac{\partial y(N)}{\partial \mu_l^o}\frac{\partial \mu_l^o}{\partial \mu_l^I}\frac{\partial \mu_l^I}{\partial \mu_j}\frac{\partial \mu_j}{\partial \sigma_j} \\ &= \begin{cases} \eta_3 \delta_j \dfrac{m_j - x_i}{(\sigma_j)^2} & if \quad m_j - \sigma_j < x_i \le m_j \\ \eta_3 \delta_j \dfrac{x_i - m_j}{(\sigma_j)^2} & if \quad m_j < x_i \le m_j + \sigma_j \end{cases}\end{aligned} \tag{22}$$

where η_2 and η_3 are the learning rates. The center of the triangle m_j and center's width of the triangle σ_j are updated according to:

$$m_j(N+1) = m_j(N) + \Delta m_j \tag{23}$$

$$\sigma_j(N+1) = \sigma_j(N) + \Delta \sigma_j \tag{24}$$

The exact calculation of the sensitivity of the system $\partial E / \partial y(N)$ which is contained in $\partial P_{inv} / \partial y(N)$ and $\partial Q_{inv} / \partial y(N)$ cannot be determined due to the uncertainties of the plant dynamic such as parameter variations and external disturbances. To overcome this problem and to increase the online learning rate of the network parameters, the delta adaptation law is adopted as:

$$\delta_o \cong e(N) + A\dot{e}(N) \tag{25}$$

where A is a positive constant.

IV. Experimentation

The block diagram of the grid-connected power inverter system for the islanding detection method is provided in Fig. 4, where C_{dc}, V_{dc}, i_{dc} are capacitor, DC link voltage and current

respectively; L_f is inductor between the power inverter and utility power; i_{us}, i_{vs}, i_{ws} are the three-phase power inverter currents; V_{un}, V_{vn}, V_{wn} are the three-phase voltages of *RLC* load; T_a, T_b, T_c are the control signals of power inverter. The switch S1 represents the utility circuit breaker. When the S1 closes, the power inverter systems operate in grid-connected mode. On the other hand, when the S1 opens, the utility power is disconnected. The parallel *RLC* resonant load represents a local load, and the *RLC* resonant frequency is designed to 60 ± 0.1*Hz*. Moreover, when the utility frequency is 60*Hz*, the *RLC* resonant load represents a resistive load. If the utility power fails and the output power of the power inverter and the *RLC* load power are balanced, without effective islanding detection method, the output voltage and frequency of the power inverter will be maintained as same as the utility power resulting in the islanding phenomenon. Therefore, this test system can be applied to determine if the islanding detection method is valid.

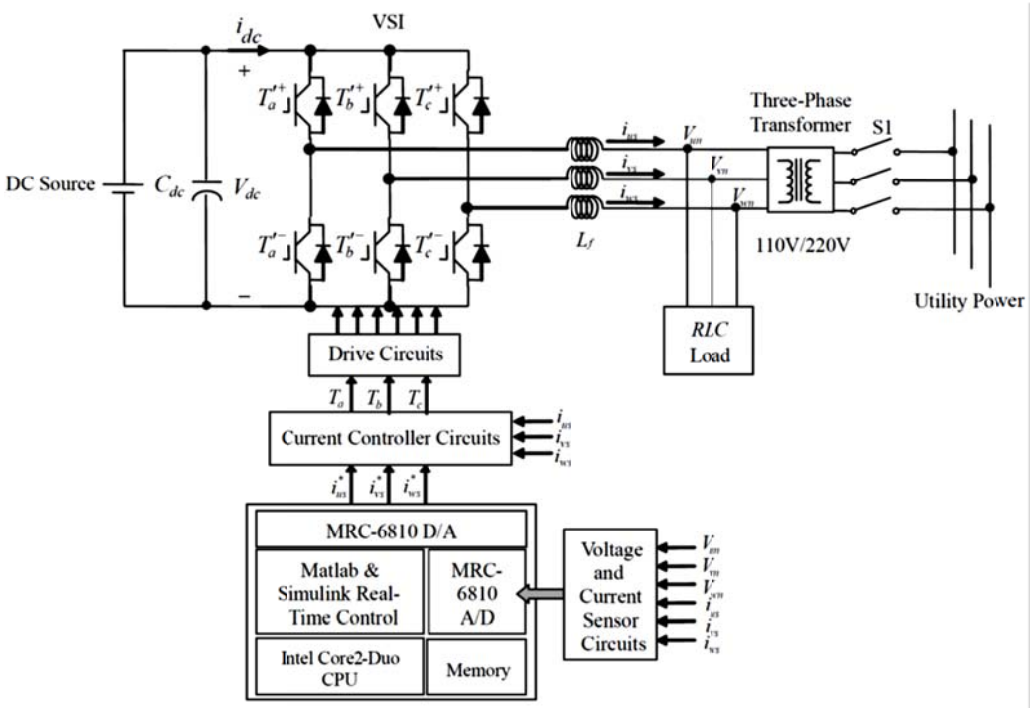

Fig. 4 Block diagram of the grid-connected power inverter system for islanding detection

In the experimentation, first, some experimental results using PI and PFNN controllers for the tracking control of the active and reactive power are demonstrated to show the control performance of the power inverter with the current injection disturbance. The experimental results of using PI controller for active power command from 0kW to 2kW and reactive power command set to be 0Var are shown in Fig. 5. In this study, the gains of the PI controller are obtained by trial and error in order to achieve good transient and steady-state control performance. The responses of active power and reactive power outputs of the power inverter are shown in Figs. 5 (a) and (b). Moreover, the experimental results using PFNN controllers for active power command from 0kW to 1kW and reactive power command set to be 0Var are shown in Fig. 6. The responses of active power and reactive power outputs of the power inverter are shown in Figs. 6 (a) and (b). From the experimental results, excellent tracking responses of both active power and reactive power can be obtained for the PFNN controller owing to the online training ability. Furthermore, the output active power and reactive power of the power inverter are not affected by the added disturbance signal. In addition, the robust control performance of the adopted PFNN controller at different operating conditions is obvious.

To verify the effectiveness of islanding detection, the utility frequency 60 Hz is designed to test the effectiveness of the proposed active islanding detection method. When the S1 shown in Fig. 4 opens, the utility power is disconnected. Fig. 7 shows the experimental results of injection disturbance method using PI controller operated at 60 Hz. The responses of frequency at the terminal of the *RLC* load and the active power output are shown in Figs. 7 (a) and (b), where P_{inv}^{*} is set to be 2kW and Q_{inv}^{*} is set to be 0Var. The utility power is disconnected at the time 1s, and the power inverter continues to deliver active power to the *RLC* load until the time 1.75s. After 1.75s, the disturbance signal is large enough to drift the frequency to shift out of the IEEE1547 scope. From Fig. 7 (a), the total time for the PI controlled power inverter stop delivering power is about 0.75s, which meets the IEEE1547 regulations (2s). Moreover, the experimental results of injection disturbance method using PFNN controller are provided in Fig. 8. The responses of frequency at the terminal of the *RLC* load and the active power output are shown in Figs. 8 (a) and (b). From the experimental results shown in Figs. 8 (a)

and (b), the total time for the PFNN controlled power inverter stop delivering power is about 0.45s, which also meets the IEEE1547 regulations. Compared with the experimental results of the proposed islanding detection method using PI controller, the responses of the proposed islanding detection method using PFNN controller are faster due to the advantages of PFNN such as online learning and quick convergence. Thus, the proposed islanding detection method using PFNN controller has excellent performance for the islanding detection.

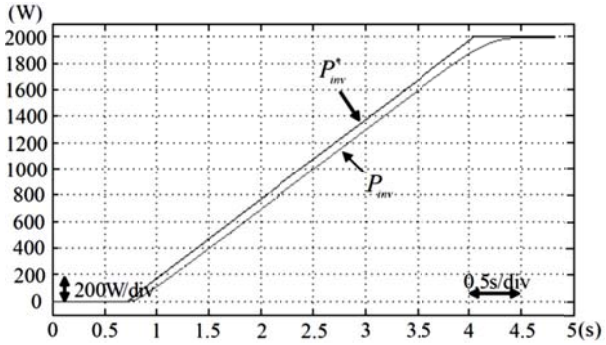

(a)

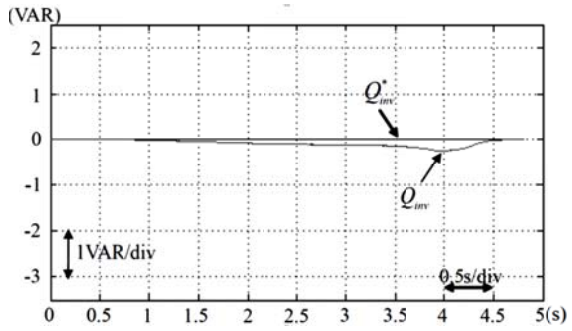

(b)

Fig. 5 Experimental results of PI controllers for tracking control, (a) responses of active power and active power command, (b) responses of reactive power and reactive power command

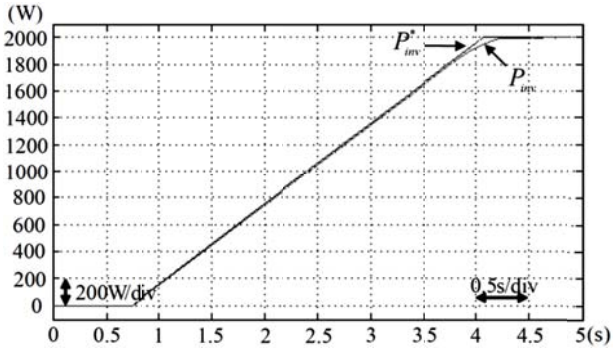

(a)

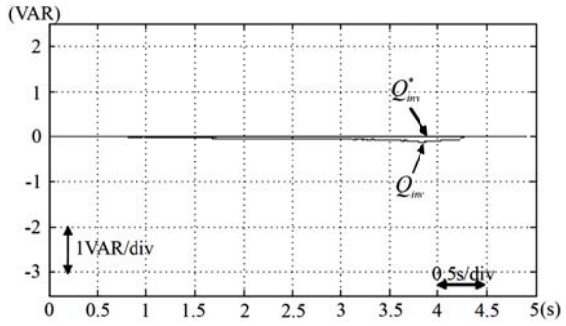

(b)

Fig. 6 Experimental results of PFNN controllers for tracking control, (a) responses of active power and active power command, (b) responses of reactive power and reactive power command

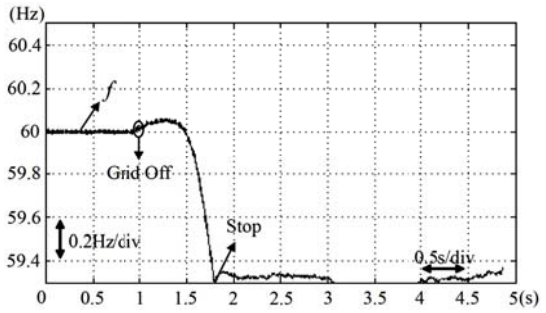

(a)

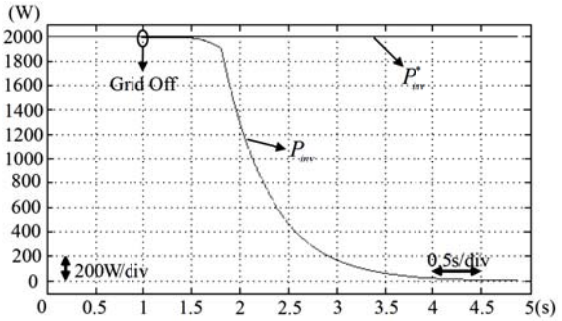

(b)

Fig. 7 Experimental results of PI controllers for proposed islanding detection, (a) frequency responses, (b) responses of active power and active power command

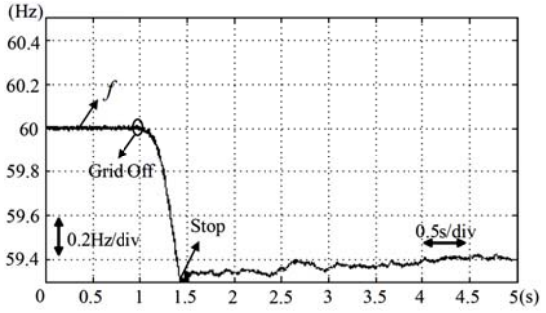

(a)

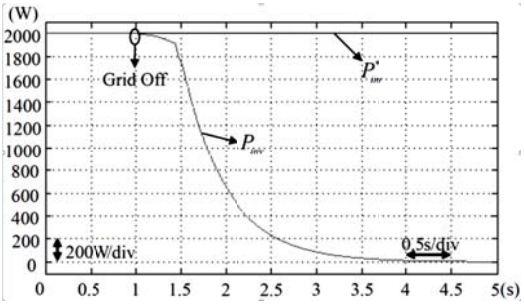

(b)

Fig. 8 Experimental results of PFNN controllers for proposed islanding detection, (a) frequency responses, (b) responses of active power and active power command

V. Conclusion

This study has successfully demonstrated the applications of the PFNN controllers on the power inverter for the tacking control of active power and reactive power outputs. Moreover, a novel islanding detection method has been successfully proposed. The proposed active islanding detection method is based on injecting a disturbance signal into the power inverter emulated the DG system through the *d*-axis current. Furthermore, the network structure and online learning algorithms of the adopted PFNN have all been described in detail. Finally, the proposed islanding detection method combined with the PFNN controller for active islanding detection has been successfully verified in the experimental results.

Acknowledgment

The author would like to acknowledge the financial support of the Ministry of Science and Technology of Taiwan through its grant MOST 103-2221-E-606-006.

References

[1] M. Ciobotaru, V. Agelidis, and R. Teodorescu, "Accurate and less-disturbing active anti-islanding method based on PLL for grid-connected PV Inverters," in *2008 Proc. IEEE Power Electronics Specialists Conf.,* pp. 4569-4576.

[2] IEEE, Std. 1547, "IEEE standard for interconnecting distributed resources with electric power systems," 2003.

[3] UL 1741, "Inverters, converters, and controllers for use in independent power systems," 2002.

[4] IEEE, Std. 929-2000, "IEEE recommended practice for utility interface of photovoltaic (PV) systems," 2000.

[5] M. E. Ropp, M. Begovic, A. Rohatgi, "Analysis and performance assessment of the active frequency drift method of islanding prevention," *IEEE Trans. Energy Conversion*, vol. 14, no.3, pp. 810–816, Sep. 1999.

[6] H. Karimi, A. Yazdani, and R. Iravani, "Negative-sequence current injection for fast islanding detection of a distributed resource unit," *IEEE Trans. Power Electronics*, vol. 23, no. 1, pp. 298–307, Jan. 2008.

[7] B. Y. Bae, J. K. Jeong, J. H. Lee, and B. M. Han, "Islanding detection method for inverter-based distributed generation systems using a signal cross-correlation scheme," *J. Power Electron*ics, vol. 10, no. 6, pp. 762–768, 2010.

[8] T. T. Ma, "Novel voltage stability constrained positive feedback anti-islanding algorithms for the inverter-based distributed generator systems," *IET Renewable Power Generation*, vol. 4, no. 2, pp. 176-185, March, 2010.

[9] F. Wang, and Z. Mi, "Passive islanding detection method for grid connected PV system," in *2009 Proc. Int. Conf. on Industrial and Information Systems*, pp. 409-412

[10] Y. Gao, and M. J. Er, "An intelligent adaptive control scheme for postsurgical blood pressure regulation," *IEEE Trans. Neural Networks,* vol. 16, no. 2, pp. 475-483, March, 2005.

[11] F. J. Lin, H. J. Shieh, P. K. Huang, and L. T. Teng, "Adaptive control with hysteresis estimation and compensation using RFNN for piezo-actuator," *IEEE Trans. Ultrasonics, Ferroelectrics, and Frequency Control*, vol. 53, no. 9, pp. 1649-1661, Sept. 2006.

[12] M. Tripathy, R. P. Maheshwari, and H. K. Verma, "Application of probabilistic neural network for differential relaying of power ransformer," *IET Generation, Transmission and Distribution*, vol. 1, no. 2, pp. 218–222, March, 2007.

[13] N. Perera, and A. D. Rajapakse, "Recognition of fault transients using a probabilistic neural-network classifier," *IEEE Trans. Power Delivery*, vol. 1, no. 26, pp. 410-419, Jan., 2011.

[14] M. Tripathy, R. P.Maheshwari, and H. K. Verma, "Power transformer differential protection based on optimal probabilistic neural network," *IEEE Trans. Power Delivery,* vol. 25, no. 1, pp. 102-112, Jan., 2010.

[15] H. X. Li, and Z. Liu, "A probabilistic neural-fuzzy learning system for stochastic modeling," *IEEE Trans. Fuzzy Systems,* vol. 16, no. 4, pp. 898-908, Aug., 2008.

[16] F. J. Lin, Y. S. Huang, K. H. Tan, Z. H. Lu, and Y. R. Chang, "Intelligent-controlled doubly fed induction generator system using PFNN," *Neural Computing and Applications*, vol. 22, no. 7-8, pp. 1695-1712, 2013.

[17] A. Yafaoui, B. Wu, and S. Kouro, "Improved active frequency drift anti-islanding detection method for grid connected photovoltaic systems," *IEEE Transactions on Power Electronics,* vol. 27, no. 5. pp. 2367-2375, May, 2012.

K. H. Tan received the B.S., M.S., and Ph.D. degrees in electrical and electronic engineering from Chung Cheng Institute of Technology (CCIT), National Defense University (NDU), Taiwan, ROC in 2002, 2007 and 2013, respectively. He has been a member of the faculty at CCIT, where he is currently an assistant professor in the Department of Electrical and Electronic Engineering. His teaching and research interests include power electronics, microgrid system and intelligent control.

C. C. Hu received the B.S. and M.S. degrees in Electrical and Electronic Engineering from Chung-Cheng Institute of Technology, Taiwan in 2002, and 2007, respectively. He was received the Ph.D. degree in Electrical Engineering from National Central University, Taiwan in 2015. He has been a deputy engineer of the System Manufacturing Center at National Chung-Shan Institute of Science and Technology, and his research interests include nanophotonics, electromagnetic field simulation, near-field optics and plasmonics.

C. W. Lan was born in Tainan, Taiwan, 1981. He received the B.S., M.S. and Ph.D. degrees from the Department of Electrical and Electronic Engineering, and the School of Defense Science, Chung Cheng Institute of Technology, National Defense University, Taoyuan, Taiwan, in 2003, 2006, and 2013, respectively. He is currently an Assistant Professor of the Department of Electrical and Electronic Engineering of Chung Cheng Institute of Technology, National Defense University. His current research interests include humanoid robot, computer vision, and remote control.

S. S. Lin received the B.S. degree and the M.S. degree from the Department of Electrical Engineering, Chung Cheng Institute of Technology (CCIT) in 1997 and 2003 respectively, and the Ph.D. degree from CCIT, National Defense University (NDU) in 2010. Currently, he is an associate professor of the Department of Electrical and Electronic Engineering, CCIT, NDU, Taoyuan, Taiwan. His current research interests include Web-based automation, RFID applications, WSN-based control and monitoring applications, power monitoring systems and microprocessor systems.

T. J. Chang received the B.S., M.S., and Ph.D. degrees in electrical and electronic engineering from Chung Cheng Institute of Technology (CCIT), National Defense University (NDU), Taiwan, ROC in 1993, 2001 and 2008, respectively. He has been a member of the faculty at CCIT, where he is currently an assistant professor in the Department of Electrical and Electronic Engineering. His teaching and research interests include operating system, information security, data structure, computer network.